Microscopic Mechanism of Solute−Solvent Energy Dissipation Probed by Picosecond Time-Resolved Raman Spectroscopy

Koichi Iwata[†] and Hiro-o Hamaguchi*[,†,‡]

Molecular Spectroscopy Laboratory, Kanagawa Academy of Science and Technology (KAST), KSP East 301, 3-2-1 Sakato, Kawasaki 213, Japan, and Department of Basic Science, Graduate School of Arts and Sciences, The University of Tokyo, 3-8-1 Komaba, Meguro, Tokyo 153, Japan

Received: July 8, 1996; In Final Form: September 30, 1996[⊗]

The excess energy dissipation process of photoexcited S_1 *trans*-stilbene in solution has been studied with picosecond time-resolved Raman spectroscopy. The peak position of the 1570-cm^{-1} band (C═C stretch) is shown to be useful as an indicator of picosecond temperature changes; a picosecond time-resolved Raman spectrometer can be regarded as a "picosecond Raman thermometer". The cooling rates of S_1 *trans*-stilbene thus observed in 10 different solvents show a strong correlation with the thermal diffusivities of the bulk solvents. Based on this observation, a simple numerical model is proposed for the solute−solvent energy dissipation process in solution. The observed cooling kinetics are analyzed with this macroscopic model. It is concluded that the excess energy is first shared among the solute and the nearest solvent molecules in a few picoseconds or faster. The further heat conduction to outer-sphere solvent molecules determines the whole dissipation rate, which explains the observed correlation between the vibrational cooling rate and the thermal diffusivity of the solvent.

Introduction

Dissipation of excess energy plays an important role in chemical reactions in solution. With the help of the energy dissipation process, newly generated product molecules can transfer to their ground states. If the products cannot release their excess energy to the surrounding solvent molecules efficiently, they might go back to the energetically equivalent activation complexes, or even to the reactant molecules. Alternatively, further reactions can proceed from the once formed primary products, which will result in different and sometimes uncontrollable final products. For example, when metal carbonyl compounds are photoexcited, their carbonyl (CO) groups often leave the parent molecules.[1] In the gas phase, depending on the photon energy of the excitation light, more than one reaction product with different number of CO groups is formed. In the solution, however, the number of leaving CO group is always one. This is because efficient excess energy dissipation takes place in solution as soon as the first CO group is lost. The excess energy dissipation process is an important and characteristic part of chemical reactions in solution.

If a molecule is photoexcited with more energy than that required for the 0−0 transition, the excess energy not used for the electronic excitation is stored in the vibrational, rotational, and translational degrees of freedom of the molecule. In solution, this excess energy is rapidly redistributed among the solute's internal degrees of freedom and is simultaneously dissipated into the surrounding solvent molecules. This dissipation process can be monitored if the amount of the excess energy still left in the solute molecule can be measured with a time resolution faster than the dissipation rate. That is, if we can measure the temperature of the solute molecule after the photoexcitation with a picosecond time resolution, we can monitor the excess energy dissipation process in solution.[2]

The temperature of photoexcited solute molecules has been estimated by using time-resolved absorption spectroscopy in the visible to the ultraviolet region.[3−5] The absorption band shapes were used as a diagnostic tool to estimate the temperatures of the solute molecule. It is also possible to use time-resolved infrared or Raman spectroscopy to estimate the temperature of molecules.[2,6−9] Because these spectroscopies directly observe the vibrational level structure and its dynamics, the interpretation of the experimental data is more straightforward.

To obtain a general conclusion on the mechanism of the excess energy dissipation, it is necessary to observe the dissipation process in various conditions. Thus far, a few groups have compared the vibrational cooling rates in different solvents.[4,8] However, to the best of our knowledge, there has been no experiment reported in which the dissipation kinetics is measured while the solvent is changed systematically.

The first excited singlet (S_1) state of *trans*-stilbene has been studied well with picosecond time-resolved Raman spectroscopy. Among several electronically excited molecules whose vibrational states have been characterized with time-resolved Raman spectroscopy, S_1 *trans*-stilbene is one of the best studied.[10] Since the first observation of its spectra,[11,12] the experimental assignment of its Raman bands,[13,14] the time and solvent dependence of the position and shape of its Raman bands,[15−21] and the relationship between its Raman band shape and the trans−cis isomerization reaction rate[22−24] have been reported. In this paper, we report the solvent dependence of the vibrational cooling kinetics of S_1 *trans*-stilbene. We present the observed strong correlation between the excess energy dissipation rate and the thermal diffusivities of the solvents. We discuss the mechanism of the dissipation process in a molecular scale and reproduce the observed dissipation kinetics by using a simple numerical model.

Experimental Section

The picosecond time-resolved Raman spectra were measured with the pump−probe method. The details of the picosecond time-resolved Raman spectrometer used in this work have been published elsewhere.[25] In short, the second harmonic of the compressed output from a cw mode-locked Nd:YAG laser

[†] KAST.
[‡] The University of Tokyo.
[⊗] Abstract published in *Advance ACS Abstracts,* December 15, 1996.

S1089-5639(96)02010-5 CCC: $14.00

(Spectra Physics, 3800S) was used to synchronously pump a mode-locked dye laser (Spectra Physics, 3520, rhodamine 6G). The dye laser output was amplified (588 nm, 2 kHz, 10−20 mW, 3.2 ps, 3.5 cm^{-1}) by using the second harmonic of a cw Nd:YAG regenerative amplifier (Spectra Physics, 3800RA) output and was frequency doubled. The obtained second harmonic (294 nm, 2 kHz, 1−5 mW) of the amplified output was used for the pump light, while the remaining visible was used for the probe. The dye laser was operated so that the probe pulse was close to its transform limit. The time delay between the pump and probe light pulses was controlled by a stepping motor driven delay line. The probe light power was decreased to 0.1 mW at the sample point in order to avoid the undesired effect on the Raman band shape caused by the high laser light field. The probe beam diameter at the sample point was approximately 40 μm. In one series of measurements, the order of the time delay was set to be random so that the possible long-term drift of the laser system would not affect the experimental data. The Raman scattered light was collected and analyzed by a single spectrograph (Instruments SA, HR 320; grating, 1800 lines/mm) and detected by a liquid nitrogen cooled CCD detector (Princeton Instruments, LN/CCD 1024 TKB). The unshifted scattered light was rejected with a narrow band rejection filter (Kaiser Optical Systems) placed in front of the entrance slit of the spectrograph.

The sample of *trans*-stilbene and the solvents (Wako Chemicals) were used as received. The concentration was 1×10^{-3} mol dm^{-3} for ethylene glycol and 3×10^{-3} mol dm^{-3} for the other solvents.

Results and Discussion

Use of the 1570-cm^{-1} Band as a Picosecond Temperature Indicator. When *trans*-stilbene is irradiated with the excitation light of 294 nm in solution, the S_1 state is formed with an excess energy of about 2800 cm^{-1}. Then, immediately after this photoexcitation, S_1 *trans*-stilbene is expected to start dissipating the excess energy to the surrounding solvent molecules. We recorded the time-resolved Raman spectra of S_1 *trans*-stilbene by changing the time delay between the pump and probe light pulses from −10 to 100 ps. In the observed time-resolved Raman spectra of S_1 *trans*-stilbene, an intense band appears around 1570 cm^{-1}. This band has been assigned to the central C═C stretch vibration.[13] The time-resolved Raman spectra in the C═C stretch region are shown in Figure 1 for a chloroform solution. The intensity of each Raman band is normalized so that the time dependence of the peak position and the band shape can be better compared. As the time delay increases, the peak position moves to the higher wavenumber. This is essentially the same time dependence as reported before for other solutions.[2,18−21]

To analyze the observed time dependence of the 1570-cm^{-1} band, we carried out a least-squares fitting using a single Lorentzian function.[18] The results are plotted in Figure 2 with filled triangles (left axis). The time-dependent change of the peak position is well fitted by a single-exponential decay function with a lifetime of 12 ps.[26] Hester et al. observed this band in a hexane solution at $t = 20$ ps while changing the solution temperature and obtained a linear relation between the peak position and the temperature.[20] Weaver et al. reported that the peak position at $t = 0$ is different depending on the excitation energy but that the positions at larger time delays are getting closer regardless of the excitation energy.[19] These reports suggest that the time-dependent change of the peak position of the 1570-cm^{-1} Raman band represents the vibrational cooling process of the S_1 *trans*-stilbene after the photoexcitation.

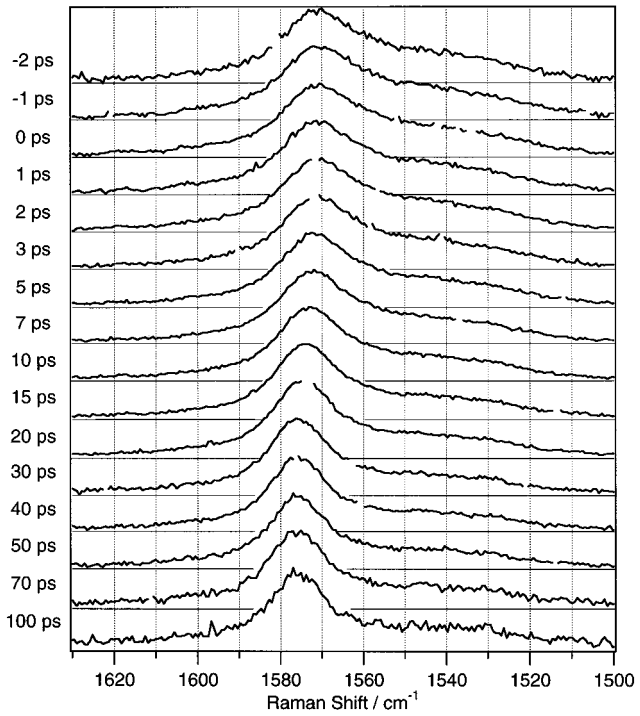

Figure 1. C═C stretch region of the time-resolved Raman spectra of S_1 *trans*-stilbene in chloroform. The pump and probe wavelengths were 294 and 588 nm. The intensity of the Raman band at each time delay is normalized.

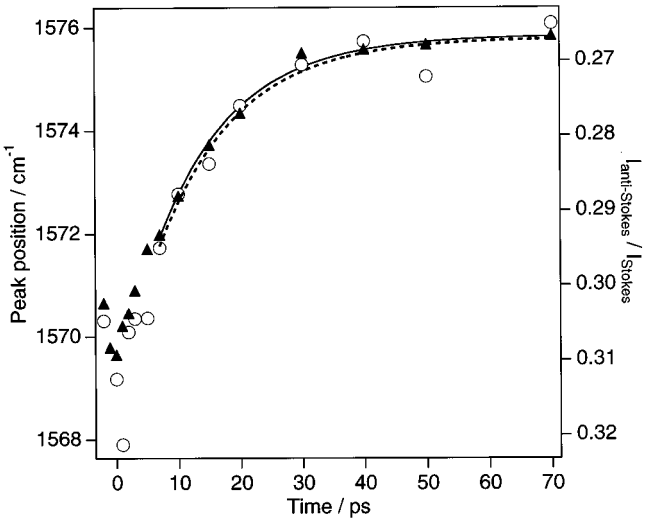

Figure 2. Time dependence of the peak position of the 1570-cm^{-1} Raman band of S_1 *trans*-stilbene in chloroform solution (filled triangle). The time dependence of the anti-Stokes/Stokes intensity ratio is also shown with open circles. The best fit of the peak position change with a single-exponential function is shown with a solid curve, while the best fit of the anti-Stokes/Stokes intensity ratio is shown with a dotted curve. The obtained lifetime for both single-exponential decay functions was 12 ps.

To further confirm that the time-dependent change of the 1570-cm^{-1} Raman band of S_1 *trans*-stilbene represents its cooling process, we measured the time-resolved Raman spectra of S_1 *trans*-stilbene at the spectrograph position which covers both the Stokes and the anti-Stokes regions at the same time (from −400 to 400 cm^{-1}). It was essential to measure the Stokes side and the anti-Stokes side in the same spectral image so that the recording conditions for both sides were exactly the same and the comparison between them was reliable. The use of a narrow band rejection filter[27] made this measurement possible. The obtained time-resolved spectra are shown in

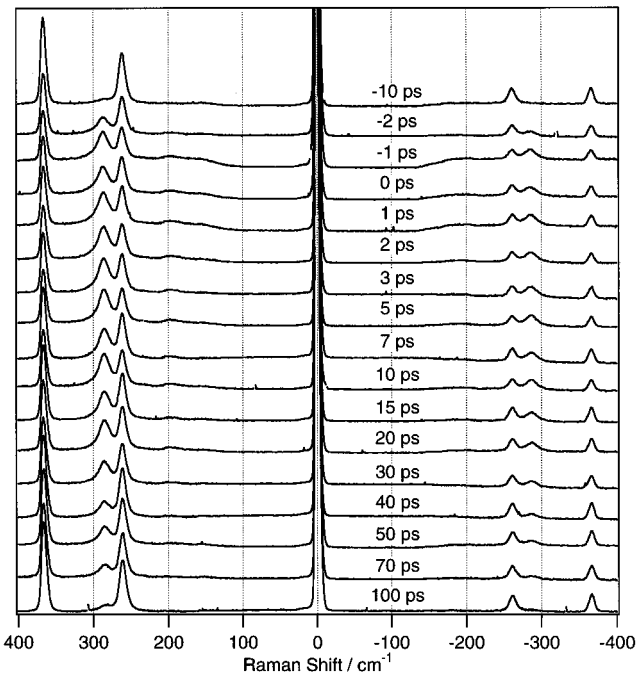

Figure 3. Low wavenumber region of the time-resolved Raman spectra of S_1 *trans*-stilbene in chloroform. The left half is for the Stokes scattering, while the right half is for the anti-Stokes scattering. The Rayleigh light is located at the center.

Figure 3. In the figure, the left half is for the Stokes scattering, while the right half is for the anti-Stokes scattering. The Rayleigh light is located at the center. The rise and decay of the Raman band from S_1 *trans*-stilbene are observed at 285 cm^{-1} for both the Stokes side and the anti-Stokes side. The two intense Raman bands at 261 and 366 cm^{-1} are from the solvent chloroform and used as internal intensity standards.

By comparing the relative intensities of the Stokes band and the corresponding anti-Stokes band, in general, we can estimate the temperature of the vibrational mode. The anti-Stokes/Stokes intensity ratio is equal to the Boltzmann factor $\exp(-E_v/kT)$, where E_v is the spacing of the vibrational levels, under an off-resonance condition (note the discussion below for resonance Raman scattering). The observed anti-Stokes/Stokes intensity ratio for the 285-cm^{-1} band of S_1 *trans*-stilbene is plotted against the time delay in Figure 2 with open circles. The anti-Stokes/Stokes intensity ratio (right axis) changes in the same way as the peak position of the 1570-cm^{-1} band does (left axis).[28] This agreement between the peak position and the anti-Stokes/Stokes intensity ratio clearly shows that the position of the 1570-cm^{-1} band can be used as an indicator of the temperature of the solute S_1 *trans*-stilbene. We can use the time-resolved Raman spectrometer as a "picosecond Raman thermometer" to monitor the cooling process of the solute molecule which directly reflects the excess energy dissipation process in solution.

As mentioned above, the anti-Stokes/Stokes intensity ratio is equal to the Boltzmann factor $\exp(-E_v/kT)$ and not to the temperature itself. We examine the relation between the Boltzmann factor and the temperature in Figure 4. In the figure, the Boltzmann factor $\exp(-E_v/kT)$ with $E_v = 285$ cm^{-1} is plotted against the temperature T with a solid curve, while the best fit to this curve by a line is shown with a dotted line. The agreement between the two is quite good. We can safely assume that the anti-Stokes/Stokes intensity ratio is linearly dependent on the factor $\exp(-E_v/kT)$ and, hence, on the temperature itself for the temperature range covered in the present study. The right axis of Figure 2 can be regarded as the temperature.

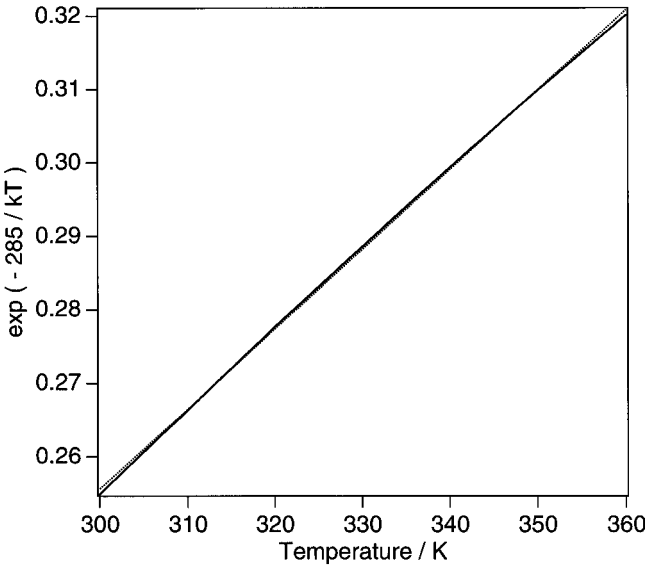

Figure 4. Relation between the Boltzmann factor $\exp(-E_v/kT)$ and temperature (solid curve). The spacing of the vibrational levels, E_v, was set to be 285 cm^{-1}. The best fit to the Boltzmann factor with a linear function is shown with a dotted line.

In Figure 2, the anti-Stokes/Stokes intensity ratio reaches the value 0.267 as the time delay increases. This ratio 0.267 corresponds to the vibrational temperature of 311 K. This value is close to room temperature. In resonance Raman scattering, however, the anti-Stokes/Stokes intensity ratio is not always equal to the factor $\exp(-E_v/kT)$, since the resonance condition can be different between the Stokes scattering and the anti-Stokes scattering. Therefore, the observed anti-Stokes/Stokes intensity ratio may not indicate the real temperature of S_1 *trans*-stilbene. It should be noted, however, that we can still obtain a reliable dissipating kinetics from the observed anti-Stokes/Stokes intensity ratio in Figure 2, even in case where the temperature derived from the ratio is shifted from the true value.

Correlation between the Solute Cooling Rate and the Solvent Thermal Diffusivity. The heat conduction and the accompanying temperature change in a macroscopic media are described by a diffusion equation,[29,30]

$$\frac{\partial U}{\partial t} = \kappa \Delta U \tag{1}$$

where U is the temperature, κ is the thermal diffusivity, and t is time. Thermal diffusivity κ is defined as

$$\kappa = \lambda / c\rho \tag{2}$$

where λ is the thermal conductivity, c is the heat capacity, and ρ is the density. When the temperature of a solute molecule is decreased, its excess energy must be released to the surrounding solvent molecules. The initial energy transfer from the solute to the nearest solvents is followed by the energy flow from the nearest solvents to the outer-sphere solvent molecules. Although the cooling itself is primarily an intramolecular process, it might be affected by the heat conduction property of the bulk solvent through this chain of energy flows. It is worth examining if the cooling rate is related to the thermal diffusivity κ of the solvent. Thus far, several groups have discussed the possible correlation between the solute cooling process and the solvent heat conduction.[4,5,21,31] Lian et al. explained the observed heating kinetics of solvent (water) by using the diffusion theory.[9] To the best of our knowledge, however, there has been no report in which the relation between the solute cooling rate and the solvent thermal diffusivity is examined in a systematic way.

TABLE 1: Thermal Diffusivity of Organic Solvents

solvent	thermal diffusivity/10^{-8} m^2 s^{-1}
heptane	8.01
chloroform	8.22
hexane	8.24
octane	8.49
decane	8.60
nonane	8.61
ethanol	8.70
toluene	8.79
ethylene glycol	9.75
methanol	10.2

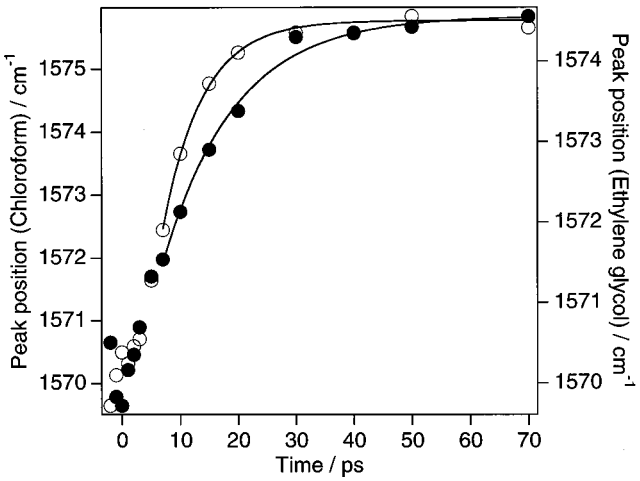

Figure 5. Observed cooling kinetics of S_1 *trans*-stilbene in ethylene glycol (open circles, right axis) and in chloroform (filled circles, left axis). The changes in the peak positions are proportional to the changes in the solute temperatures. The lifetimes of the temporal changes were obtained to be 7 ps for ethylene glycol and 12 ps for chloroform.

The thermal diffusivities of 10 organic solvents are listed in Table 1. The listed values of thermal diffusivity were calculated from the thermal conductivity,[32] specific heat,[33] and density[33] for 300 K by using formula 2. The time-resolved Raman spectra of S_1 *trans*-stilbene were measured in all the listed solvents. It was found that the cooling kinetics is in fact different depending on the thermal diffusivity of the solvent. An example of the marked difference in the observed cooling rates of S_1 *trans*-stilbene in two solvents is shown in Figure 5. The figure shows the time dependence of the peak position of the 1570-cm^{-1} band in ethylene glycol and chloroform. As in Figure 2, the peak position is proportional to the solute temperature. It is clear that the cooling rate of S_1 *trans*-stilbene is faster in ethylene glycol, which has a thermal diffusivity of 9.75×10^{-8} m^2 s^{-1}. The decay lifetime is found to be 7 ps. In chloroform, whose thermal diffusivity is 8.22×10^{-8} m^2 s^{-1}, the solute is cooled with a longer lifetime of 12 ps.

The cooling kinetics in each solvent listed in Table 1 was analyzed by the method described thus far using the exponential fittings.[26] The results are summarized in Figure 6. In Figure 6, the observed cooling rate constants are plotted against the thermal diffusivities of the solvents. There is a clear positive correlation between the cooling rate and the thermal diffusivity. A similar tendency has been reported by other groups for a smaller number of solvents.[4,8,31]

From this experiment, it is obvious that the cooling rate of S_1 *trans*-stilbene is correlated with the thermal diffusivity of the solvent. However, the reason for the observed correlation is not quite evident. The cooling is mainly happening at the solute, while the thermal diffusivity is a purely bulk property of the solvent. The cooling rate of the solute molecule might be affected by the character and the strength of the solute−solvent interaction but does not have to be controlled by the thermal diffusivity, which has no relation with the solute. Therefore, to account for the observed correlation, we assume the following molecular mechanism of the energy dissipation process in solution. In our model, the excess energy generated at the solute molecule at $t = 0$ is shared among the solute and the nearest solvent molecules almost instantaneously. Then, the excess energy flows into the bulk solvent following the macroscopic heat conduction property of the solvent. Because the initial energy redistribution among the solute and the nearest solvents is much faster than the bulk heat conduction, the excess energy trapped among the solute and the nearest solvents can only dissipate to outer-sphere solvents with a slower rate of solvent heat conduction. The entire dissipation rate is not affected by the solute−solvent interaction. It is determined by the heat conduction process in the bulk solvent, which is well characterized by the thermal diffusivity.

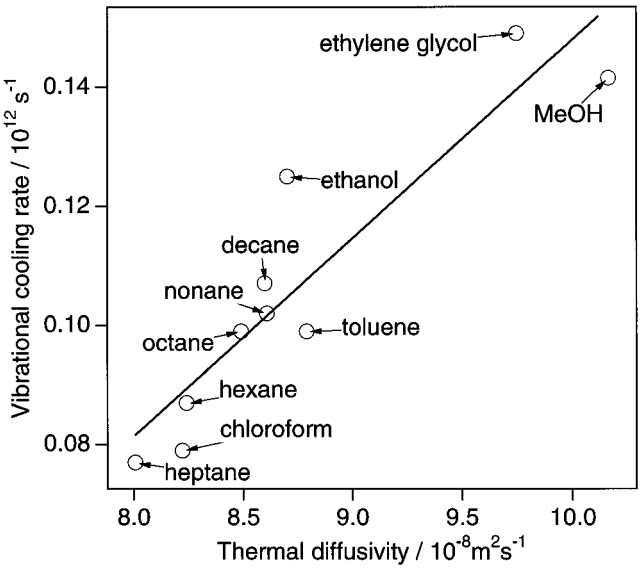

Figure 6. Relation between the observed cooling rate of S_1 *trans*-stilbene and the thermal diffusivity of the solvent. There is a clear correlation between the two.

As mentioned in the previous paragraph, the excess energy moves across two different types of interfaces during the dissipation process. One is the solute−(nearest) solvent interface, and the other is the solvent−solvent interface. Our energy dissipation model implies that the molecular interaction is larger at the first interface than at the second one. It is most likely that *trans*-stilbene is more sensitive to the microscopic environment in the S_1 state compared to the ground state, as suggested before.[22]

Numerical Model of the Dissipating Process and Analysis of the Observed Cooling Kinetics. In this section, the observed cooling kinetics is explained quantitatively based on a simple but effective numerical model of the energy dissipation process in solution. The macroscopic heat conduction is expressed by a diffusion equation of heat (eq 1). The solution of the equation is[29,30]

$$U(x,y,z,t) = (4\pi\kappa t)^{-3/2} \int\int\int f(\xi,\eta,\zeta) \exp(-[(x-\xi)^2 + (y-\eta)^2 + (z-\zeta)^2]/4\kappa t)\, d\xi\, d\eta\, d\zeta \quad (3)$$

where $f(x,y,z)$ is the initial distribution of the heat,

$$f(x,y,z) = U(x,y,z,0) \quad (4)$$

Formula 3 means that the entire time and space dependence of the temperature is determined if the initial heat distribution

$f(x,y,z)$ is known. We use two initial heat distributions and examined if either of the corresponding two solutions (3) can explain the observed cooling kinetics. The initial conditions we chose are

$$f(x,y,z) = U_a\delta(x)\delta(y)\delta(z) \quad (5)$$

and

$$f(x,y,z) = U_b \quad (|x| \le (a + r_0),\ |y| \le (b + r_0),\ |z| \le (c + r_0))$$
$$0 \quad (|x| > (a + r_0) \text{ or } |y| > (b + r_0) \text{ or } |z| > (c + r_0)) \quad (6)$$

With condition 5, we assume that all the excess energy is concentrated at the coordinate origin (center of the solute) at $t = 0$ (δ-function model). With condition 6, on the other hand, we assume that the excess energy is initially distributed equally inside a box (box model). In the box model, the *trans*-stilbene molecule is modeled as a box of dimensions $2a \times 2b \times 2c$ and the thickness of the nearest solvent layer is represented by r_0. In the following analysis, the values for a, b, and c are set to be 0.65, 0.35, and 0.1 nm. The thickness r_0 is used as a fitting parameter.

For the δ-function model, the solution for the diffusion equation (1) is

$$U(x,y,z,t) = (4\pi\kappa t)^{-3/2}U_a \exp(-[x^2 + y^2 + z^2]/4\kappa t) \quad (7)$$

while for the box model, the solution is

$$U(x,y,z,t) = U_b/8 \times \{\mathrm{erf}((a + r_0 - x)/(4\kappa t)^{1/2}) + \mathrm{erf}((a + r_0 + x)/(4\kappa t)^{1/2})\} \times \{\mathrm{erf}((b + r_0 - y)/(4\kappa t)^{1/2}) + \mathrm{erf}((b + r_0 + y)/(4\kappa t)^{1/2})\} \times \{\mathrm{erf}((c + r_0 - z)/(4\kappa t)^{1/2}) + \mathrm{erf}((c + r_0 + z)/(4\kappa t)^{1/2})\} \quad (8)$$

Therefore, the temperature at the center of the solute molecule can be expressed as

$$U(0,0,0,t) = U_a(4\pi\kappa t)^{-3/2} \quad (9)$$

for the δ-function model and

$$U(0,0,0,t) = U_b\{\mathrm{erf}((a + r_0)/(4\kappa t)^{1/2})\} \times \{\mathrm{erf}((b + r_0)/(4\kappa t)^{1/2})\} \times \{\mathrm{erf}((c + r_0)/(4\kappa t)^{1/2})\} \quad (10)$$

for the box model.

By using formulas 9 and 10 as model functions, we try to reproduce the observed cooling kinetics of S_1 *trans*-stilbene in the hexane solution. The results are shown in Figure 7. In the figure, the observed peak positions for the 1570-cm^{-1} band (upper half) and the 1180-cm^{-1} band (lower half) are plotted against the time delay. The fitting with the model function (9) is shown with a dashed curve for the 1570-cm^{-1} band, and the fittings with (10) are shown with solid curves for the 1570-cm^{-1} and 1180-cm^{-1} bands. If the δ-function model is used, the agreement between the model and the observation is poor. However, the model function for the box model agrees well with the observation. The best fit was obtained when the thickness $r_0 = 1.25$ nm for the 1570-cm^{-1} band and 1.32 nm for the 1180-cm^{-1} band. These results for the box model agree with our previous analysis in which a cube with 1.6 nm was assumed for the initial heat distribution.[2]

The conclusion we reached in the previous section is supported here by the fact that the cooling kinetics with the δ-function model does not reproduce the observed data, while the box model reproduce the observation very well. The excess energy is shared with the solute and the nearest solvents at a very early stage of the dissipation process, and then the "slow" energy flow into the bulk solvent follows. At the present point, we do not know exactly how fast the initial heat redistribution among the solute and the nearest solvents takes place. Judging from the time resolution of our experimental apparatus, however, the longest possible time needed for the event to occur is a few picoseconds. This is in agreement with earlier observations on the solute−solvent energy transfer.[9,31] A schematic diagram representing the present energy dissipation model is shown in Figure 8.

It should be noted that the two different vibrational modes, 1570 and 1180 cm^{-1}, show essentially the same time dependence in Figure 7. This result agrees with our previous report.[18]

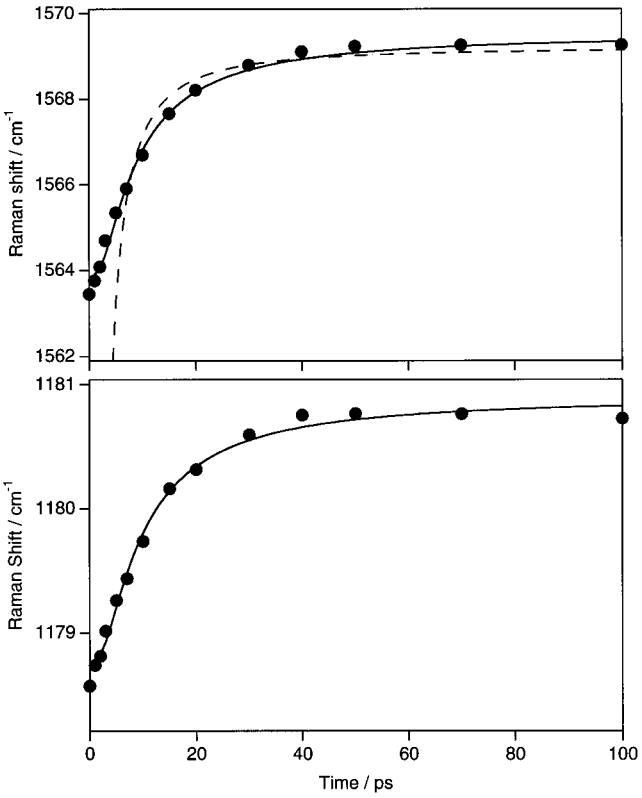

Figure 7. Observed cooling kinetics of S_1 *trans*-stilbene in hexane solution and its reproduction by using a simple numerical model (see the text for the details). The model function with the initial heat distribution of δ-function is shown in the upper half with a dashed curve, while the simulated kinetics for the initial heat distributions of boxes are shown as solid curves. There is little difference between the upper half (for 1570-cm^{-1} band) kinetics and the lower half (1180-cm^{-1} band) kinetics.

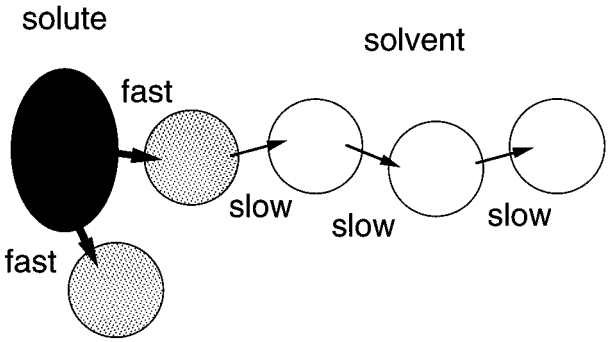

Figure 8. Schematic diagram of the molecular mechanism of the solute−solvent energy dissipation process.

In this study, however, it also became clear that the same kinetics can describe the time dependence of the vibrational temperature of the 285-cm^{-1} mode. We have found no experimental evidence which shows that the excess energy is not distributed statistically among the S_1 *trans*-stilbene vibrational degrees of freedom, at least after a few picoseconds of the photoexcitation. This contrasts with recent reports by Matousek et al.[28] and Qian et al.[34] In the higher wavenumber region, we did not observe the anti-Stokes signals which indicate a nonstatistical distribution among vibrational degrees of freedom. The reason for this apparent disagreement is not clear now.

Currently we are trying to determine the number of nearest solvents around S_1 *trans*-stilbene which receive the excess energy at the early stage of dissipation. This information will be valuable in understanding the dynamic structure of solution as well as in connecting the fruitful results from the cluster chemistry to the solution chemistry.

Conclusions

The excess energy dissipation process from S_1 *trans*-stilbene after the photoexcitation was monitored with picosecond time-resolved Raman spectroscopy. By comparing the time dependence of the peak position of the 1570-cm^{-1} band and the anti-Stokes/Stokes intensity ratio, we confirmed that the position of the 1570-cm^{-1} band can be used as a picosecond temperature indicator. The excess energy dissipation processes in 10 different solvents were examined by monitoring the cooling kinetics of the S_1 *trans*-stilbene through the 1570-cm^{-1} peak position. The observed cooling rates show a strong correlation with the thermal diffusivities of the solvents. It is assumed that the entire energy dissipation rate is controlled by the heat conduction rate in the bulk solvent because it is slower than the energy transfer from the solute to the nearest solvents.

To explain the observed cooling kinetics quantitatively, we have made a simple but effective numerical model based on the macroscopic diffusion of heat. If we assume that the excess energy is distributed equally inside a box which is larger than *trans*-stilbene, then the observed cooling kinetics is well reproduced by this model. This is consistent with the observed dependence of the solute cooling rate on the thermal diffusivity of the solvent. The excess energy is shared with the solute and the nearest solvents at the very early stage of the dissipation process. This initial energy redistribution among the solute and the nearest solvents should occur in a few picoseconds or faster.

References and Notes

(1) Poliakoff, M.; Weitz, E. *Adv. Organomet. Chem.* **1986**, *25*, 277.
(2) Iwata, K.; Hamaguchi, H. *J. Mol. Liq.* **1995**, *66/66*, 417.
(3) Astholz, D. C.; Brouwer, L.; Troe, J. *Ber. Bunsenges. Phys. Chem.* **1981**, *85*, 559.
(4) Hirata, Y.; Okada, T. *Chem. Phys. Lett.* **1991**, *187*, 203.
(5) Elsaesser, T.; Kaiser, W. *Annu. Rev. Phys. Chem.* **1991**, *42*, 83.
(6) Laubereau, A.; Kaiser, W. *Rev. Mod. Phys.* **1978**, *50*, 607.
(7) Lingle, R., Jr.; Xu, X.; Zhu, H.; Yu, S.-C.; Hopkins, J. B.; Straub, K. D. *J. Am. Chem. Soc.* **1991**, *113*, 3992.
(8) Phillips, D. L.; Rodier, J.-M.; Myers, A. B. *Chem. Phys.* **1993**, *175*, 1.
(9) Lian, T.; Locke, B.; Kholodenko, Y.; Hochstrasser, R. M. *J. Phys. Chem.* **1994**, *98*, 11648.
(10) Hamaguchi, H.; Gustafson, T. L. *Annu. Rev. Phys. Chem.* **1994**, *45*, 593.
(11) Gustafson, T. L.; Roberts, D. M.; Chernoff, D. A. *J. Chem. Phys.* **1983**, *79*, 1559.
(12) Hamaguchi, H.; Kato, C.; Tasumi, M. *Chem. Phys. Lett.* **1983**, *100*, 3.
(13) Hamaguchi, H.; Urano, T.; Tasumi, M. *Chem. Phys. Lett.* **1984**, *106*, 153.
(14) Urano, T.; Hamaguchi, H.; Yamanouchi, M.; Tsuchiya, S.; Gustafson, T. L. *J. Chem. Phys.* **1989**, *91*, 3884.
(15) Hamaguchi, H. *Chem. Phys. Lett.* **1986**, *126*, 185.
(16) Hamaguchi, H. *J. Chem. Phys.* **1988**, *89*, 2587.
(17) Kamalov, V. F.; Koroteev, N. I.; Shkurinov, A. P.; Toleutaev, B. N. *Chem. Phys. Lett.* **1990**, *147*, 335.
(18) Iwata, K.; Hamaguchi, H. *Chem. Phys. Lett.* **1992**, *196*, 462.
(19) Weaver, W. L.; Huston, L. A.; Iwata, K.; Gustafson, T. L. *J. Phys. Chem.* **1992**, *96*, 8956.
(20) Hester, R. E.; Matousek, P.; Moore, J. N.; Parker, A. W.; Toner, W. T.; Towrie, M. *Chem. Phys. Lett.* **1993**, *208*, 471.
(21) Qian, J.; Schultz, S. L.; Bradburn, G. R.; Jean, J. M. *J. Phys. Chem.* **1993**, *97*, 10638.
(22) Hamaguchi, H.; Iwata, K. *Chem. Phys. Lett.* **1993**, *208*, 465.
(23) Deckert, V.; Iwata, K.; Hamaguchi, H. *J. Photochem. Photobiol. A*, in press.
(24) Hamaguchi, H. *Mol. Phys.*, in press.
(25) Iwata, K.; Yamaguchi, S.; Hamaguchi, H. *Rev. Sci. Instrum.* **1993**, *64*, 2140.
(26) Single-exponential decay functions are used as phenomenological formulas here. Although they are not the exact solutions of the diffusion equation (1), a real solution (eq 10) can be well fitted with an exponential decay function. By using the decay rate constant of the exponential function, we can describe the cooling kinetics quite effectively. Therefore, we fit the observed cooling kinetics with an exponential decay function and use the decay rate constant as a single parameter to characterize the kinetics.
(27) Yang, B.; Morris, M. D.; Owen, H. *Appl. Spectrosc.* **1991**, *45*, 1533.
(28) Matousek, P.; Parker, A. W.; Toner, W. T.; Towrie, M.; de Faria, D. L. A.; Hester, R. E.; Moore, J. N. *Chem. Phys. Lett.* **1995**, *237*, 373.
(29) Carslaw, H. S.; Jaeger, J. C. *Conduction of Heat in Solids*, 2nd ed.; Oxford University: Oxford, 1959.
(30) Crank, J. *The Mathematics of Diffusion*, 2nd ed.; Oxford University: Oxford, 1975.
(31) Nikowa, L.; Schwarzer, D.; Troe, J. *Chem. Phys. Lett.* **1995**, *233*, 303.
(32) Touloukian, Y. S.; Liley, P. E.; Saxena, S. C. *Thermal Conductivity, Nonmetallic Liquids and Gases. The TPRC Data Series, Thermophysical Properties of Matter Vol. 3*; IFI/Plenum Data: New York, 1970.
(33) Touloukian, Y. S.; Makita, T. *Specific Heat, Nonmetallic Liquids and Gases. Thermophysical Properties of Matter, The TPRC Data Series Vol. 6*; IFI/Plenum Data: New York, 1970.
(34) Qian, J.; Schultz, S. L.; Jean, J. M. *Chem. Phys. Lett.* **1995**, *233*, 9.